Intl. J. River Basin Management Vol. 6, No. 2 (2008), pp. 149–162

Quantification of uncertainties in flood risk assessments

HEIKO APEL*, BRUNO MERZ and ANNEGRET H. THIEKEN, *GeoForschungsZentrum Potsdam (GFZ), Section Engineering Hydrology, Telegrafenberg, 14473 Potsdam, Germany. *E-mail: hapel@gfz-potsdam.de (author for correspondence)*

ABSTRACT
By a common definition, flood risk assessments are comprised of two parts: a hazard and vulnerability assessment. The hazard assessment investigates the extent and magnitude of usually large flood events, which are associated to a certain exceedance probability, whereas the vulnerability part assesses the impact of the flooding on specified targets, e.g., building, people or infrastructure. Being inherently speculative flood risk assessments should always be accompanied by an uncertainty assessment in order to assist consequent decision properly. In this paper a dynamic-probabilistic method is proposed, which enables a cumulated flood risk assessment of a complete river reach considering dike failures at all dike locations. The model uses simple but computational efficient modules to simulate the complete process chain of flooding. These modules are embedded into a Monte Carlo framework thus enabling a risk assessment which is physically based thus mapping the real flooding process, and which is also probabilistic and not based on scenarios. The model also provides uncertainty estimates by quantifying various epistemic uncertainty sources of the hazard as well as the vulnerability part in a second layer of Monte Carlo simulations. These uncertainty estimates are associated to defined return intervals of the model outputs, i.e., the derived flood frequencies at the end of the reach and the risk curves for the complete reach, thus providing valuable information for the interpretation of the results. By separating single uncertainty sources a comparison of the contribution of different uncertainty sources to the overall predictive uncertainty in terms of derived flood frequencies and monetary risks could be performed. This revealed that the major uncertainties are extreme value statistics, resp. the length of the data series used and the discharge-stage relation used for the transformation of discharge into water levels in the river.

Keywords: Flood risk assessment; dynamic-probabilistic model; uncertainty analysis; Monte Carlo analysis.

1 Introduction

Commonly, flood risk is defined as the exceedance probability of events of a given magnitude and a given loss. Therefore, risk is commonly defined as a composition of two aspects, hazard and vulnerability. However, it has to be noted that other definitions exist (Kelman, 2002), but in the context of this work the described definition is used. Flood hazard is described by the exceedance probability of damaging flood situations in a given area and within a specified period of time, and by the characteristics of the flood situations (e.g., extent and depth of inundation). The impact of floods on society is quantified by its vulnerability. Usually, vulnerability is expressed by the exposure of people and assets to floods, and by the susceptibility of these elements at risk to suffer from flood damage (e.g., Merz and Thieken, 2004). Comprehensive risk assessments that take into account the hazard and the vulnerability aspect of flood risk are gaining more and more attention in the fields of flood design and flood risk management. By quantifying the flood risk, they allow to better prepare for disasters. They are an essential element for the appraisal of cost-effectiveness of prevention measures and for optimised investments.

Risk assessments always contain probabilities as result of the inability to deterministically forecast future damage events. Therefore, uncertainty is a characteristic aspect of risk assessments (e.g., Carrington and Bolger, 1998). However, many risk assessments do not take into account the associated uncertainties, and the reliability of such assessments cannot be judged (Amendola, 2001; Felter and Dourson, 1998). In such cases the recipients of risk analyses, such as spatial planners, disaster managers or municipal administrations, tend to assume that the results of risk analyses are correct, e.g., the 500-year flood, its inundation area and the calculated losses are used without reflections about their reliability. Or, in case awareness about uncertainties of these assessments is present, the lack of quantifications of the uncertainties leaves often no choice but to use these assessment as they are.

Risk assessments that are accompanied by an indication of the reliability of the risk quantifications are a much better basis for decision-making. Optimal decisions can only be expected when all relevant uncertainties are taken into consideration (USACE, 1992; Aven and Pörn, 1998). The lack of quantitative characterisation of uncertainty may yield a qualitatively and quantitatively different answer than that derived from a reasoned treatment of uncertainty (Morgan and Henrion, 1990; Frank, 1999). Zerger *et al.* (2002) give an example how an uncertainty indication may influence prevention strategies. The analysis of the storm surge risk in Cairns, Australia, showed that, due to small topographic

Received on May 4, 2007. Accepted on November 16, 2007.

gradients, small errors in the digital elevation model may lead to large deviations in the predicted inundation area. In such a case, where only very uncertain statements can be made, it may not be sufficient to display flooded and safe areas. It may be necessary to prepare for the situation that the risk analysis underestimates the real, but unknown risk. Furthermore, the level of uncertainty can help guide the boldness of a decision. For example, people are more willing to accept an irreversible decision if its uncertainty is low (Moore and Brewer, 1972).

Another important argument for uncertainty assessments is the insight in the system under study that can be gained from comprehensive uncertainty analyses. The question whether the available information suffices to make an informed decision, or whether additional information has to be collected, cannot be answered without an estimation of the associated uncertainty. Further, the consideration of different uncertainty sources and of their respective contribution to the overall uncertainty may guide additional investments for better information (Haimes *et al.*, 1994): The largest gain in terms of uncertainty reduction is obtained when information is collected for the uncertainty source with the largest reduction of the overall uncertainty. Risk assessments are usually based on many assumptions. Uncertainty analyses illustrate the implications of different assumptions, and, thus, help to improve the underlying models in order to yield more reliable results.

Due to their speculative nature, risk assessments are approximations for the unknown risk. Usually, assessments of extreme events and their consequences cannot be validated in the traditional sense (Hall and Anderson, 2002). Since risk assessments contain statements about events that have not been observed before, the traditional way of comparing observed and simulated data is not or only partially applicable. Uncertainty analyses are one way for alternative validation: Quantifying the overall uncertainty and the effects of different uncertainty sources helps to judge the plausibility of the risk assessment. In case of highly uncertain model elements, i.e., sources of large uncertainties, the appropriateness of the selected approaches or data has to be questioned, or the plausibility of the results, if the model and data selection is appropriate.

There are comprehensive taxonomies of uncertainty in the literature which discuss different sources and kinds of uncertainty in detail (e.g., Morgan and Henrion, 1990; Haimes, 1998).

For the purpose of this paper, it is important to recognise two basic kinds of uncertainty that are fundamentally different from each other: natural and epistemic uncertainty. Natural uncertainty stems from variability of the underlying stochastic process, whereas epistemic uncertainty results from incomplete knowledge about the system under study (Tang and Yen, 1972; Morgan and Henrion, 1990; Plate, 1992, 1993; Hoffmann and Hammonds, 1994; NRC, 1995, 2000; Ferson and Ginzburg, 1996; Zio and Apostolakis, 1996; Haimes, 1998; Cullen and Frey, 1999; van Asselt and Rotmans, 2002). It is often stated that natural uncertainty is a property of the system, whereas epistemic uncertainty is a property of the analyst (Cullen and Frey, 1999). Different analysts, with different states of knowledge, different resources for obtaining data etc., may have different levels of epistemic uncertainty regarding their predictions. The central issue is that the differentiation in natural and epistemic uncertainty separates uncertainty which can be reduced (epistemic uncertainty) and uncertainty which is not reducible (natural uncertainty).

There are many examples for uncertainty considerations of flood hazard assessments (for a review see (Pappenberger *et al.*, 2005b). Much less has been done on the uncertainty of flood loss estimation. Examples are the study of Jonkman *et al.* (2002) concerning the number of fatalities due to large-scale flooding in The Netherlands or the uncertainty analysis of Merz *et al.* (2004a) concerning direct economic flood damage to buildings. Systematic analyses of the uncertainty of comprehensive flood risk analyses, considering both aspects of flood risk, i.e., the hazard and the vulnerability part, are rare. One example is given by (Hall *et al.*, 2005a).

The purpose of this paper is threefold. One aim is to develop a method for assessing the flood risk along river reaches in a comprehensive way, including the identified uncertainty sources in the hazard and in the vulnerability estimation. The method is developed for a 150 km reach of the Lower Rhine, however, it can be transferred to other river reaches. The second aim is to quantify the contributions of the different sources of uncertainty, thus helping to demonstrate where the largest uncertainty reduction of the risk assessment can be gained by improved process understanding or modelling techniques. The third aim is to compare the uncertainty reducing effect of additional information in order to enhance the data base for the risk assessment. Since former studies (e.g., Merz *et al.*, 2002) have shown that the uncertainty of the flood frequency analysis contributes a large share to the overall uncertainty, the uncertainty reducing effect is analysed by using two discharge series (30-years-series and a synthetic series extended to 1000 years) for the flood frequency analysis.

The flood risk assessment approach presented here is based on the works of Apel *et al.* (2004, 2006), who presented a dynamic probabilistic model system to assess flood risks and associated uncertainties. However, the present work presents some significant changes to the prior model versions. The most significant is the extension of the dike failure testing from two selected sites to a quasi continuous testing along the complete reach, thus enabling realistic cumulated flood risk assessments for the complete reach. In Apel *et al.* (2008) the effect of such a system on the flood frequency distribution at downstream gauges of the river reach was investigated. It could be shown that the model system gave more realistic estimates of the magnitude of large floods, because it could consider the retention effect of dike failures and inundated hinterlands on the discharges downstream. This cannot be achieved by a classical approach using extreme value statistics based on relatively short time series without inherent information about dike breach effects.

Additionally the uncertainty assessment has been revised and adapted to the extended model system. In comparison to the first uncertainty analysis (Apel *et al.*, 2004) the analysis presented here also considers uncertainties in the inundation estimation and damage assessment to residential buildings. Also, in the former model version the uncertainty caused by dike breach widths was not incorporated in the uncertainty assessment, but considered by

different scenarios. This has been revised in the present model version.

2 Investigation area

This study was applied to a reach of the Lower Rhine in the federal state Northrhine-Westphalia, Germany. The study reach starts at the gauge Cologne (Rhine-km, 688) and ends at the gauge Rees (Rhine-km, 837) near the Dutch-German border. Within this reach two major tributaries, the rivers *Ruhr* and *Lippe*, join the Rhine from the East. Both tributaries were considered in this study (Fig. 1). The width of the Lower Rhine is 300–400 m at mean water, with a bottom slope of 0.002.

Along the Lower Rhine the population density as well as the accumulation of large industry is one of the highest in Germany resulting in a huge damage potential. Consequently almost the complete reach is protected by dikes, except the rare areas where high natural river banks are present. The dike lines are in general parallel to the river course and amount to 330 km in total within the reach. The engineering standard of the dikes is up to date, i.e., zonated dikes with a protection aim of 500 years were built all along the reach within the last decades. This construction type reduces possible failure mechanisms to failure caused by overtopping and ship accidents or sabotage.

Because of the high population and industrial density the damage potential is.

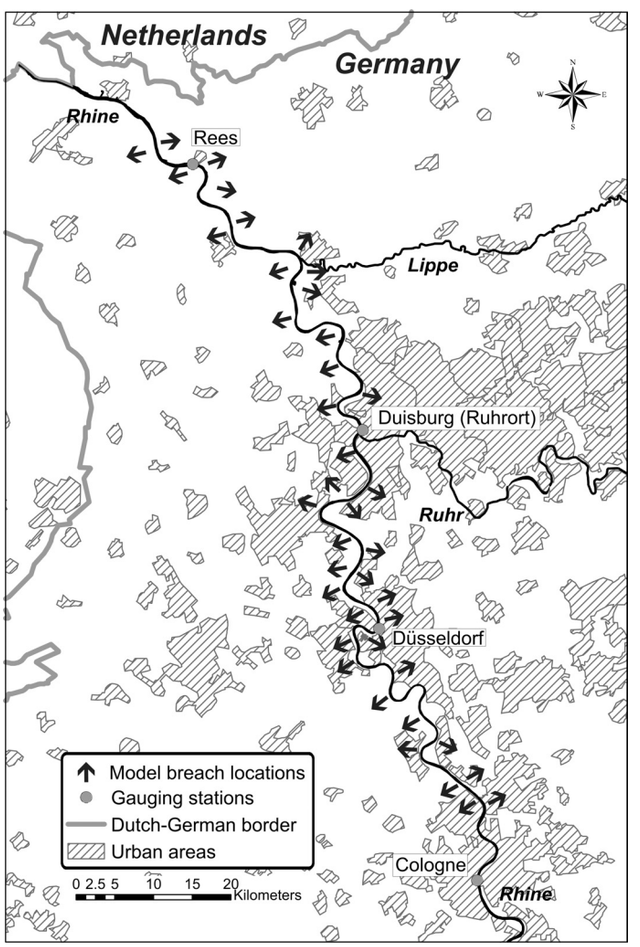

Figure 1 The investigation area Lower Rhine in North-Rhine Westphalia, Germany.

3 Dynamic probabilistic model setup

Apel *et al.* (2004, 2006) proposed a dynamic-probabilistic modelling system for the calculation of flood risks of a complete river reach. The system is comprised of simple but computational efficient modules each representing a link in the flood process chain. This process oriented model approach allows a realistic modelling of floods, including flood wave routing, test for dike breaches, reduction of flood peaks by dike breaches and finally an estimation of the inundated area and associated damage. With the exception of the module "Hydraulic transformation", all modules contain probabilistic elements. This approach reflects the inherent variability of flood processes and our inability to deterministically describe such processes as the superposition of flood peaks of the Rhine and its tributaries. Because of the computational efficiency of the system it can be embedded into a Monte Carlo simulation framework evaluating a large number of flood scenarios, which serve as the basis for the assessment of flood risks of a complete river reach. Additionally the model structure also allows an uncertainty assessment of the risk estimates by calculating uncertainty distributions for defined quantiles of the resulting risk curves.

However, prior to this publication the problem of dike breaching was only partially covered in the model, because breaching was restricted to a small number of predefined breach locations. This does not represent the real situation where breaches could occur everywhere along the reach. Since the breach location has a significant influence on the damage, the risk assessments performed with the old model can only be regarded as case studies. In order to overcome this weakness, a method was developed which enables a test for dike failures along the complete reach.

The chain of modules is listed below, separated into the hazard and vulnerability part of the risk assessment:

Hazard 1. Hydrological input (upstream boundary):
A synthetic flood wave is generated for the gauge Cologne by normalised hydrographs scaled to randomly drawn peak discharges and at gauge Cologne.

Hazard 2. Tributary input:
The inflows of the main tributaries Ruhr and Lippe to the Rhine were considered by retaining the correlation between discharges and hydrographs in the tributaries to the Rhine.

Hazard 3. Discharge – Stage relation:
This module calculates water levels in the river reach for given discharges.

Hazard 4. Dike failure and breach outflow:
The probability of a dike breach caused by overtopping is given by a two-dimensional dike fragility curve. The breach probability is conditioned on the overtopping height and duration. In

case of a breach the outflow through the reach and the reduction of the flood wave in the main channel is determined.

Vulnerability 1. Estimation of inundation depths and areas: The estimation of the inundation areas and depths are determined by the calculated outflow volume and lookup tables relating outflow volume to inundation depths and extend.

Vulnerability 2. Damage estimation The damage estimation is restricted to residential buildings only. It is performed using a simple stage-damage degree relationship. The damage degree is converted into monetary damage figures using mean asset values.

The following sections give a short description of the modules of the system, with an emphasis on the newly developed dike breach and inundation module. Detailed information about the existing modules can be found in Apel *et al.* (2004, 2006, 2008).

3.1 Hydrological input at Cologne

The input, i.e., the upstream boundary of the system is defined by a flood peak value, and a typical normalised flood hydrograph, which is scaled to the flood peak. For the generation of the flood peak discharge extreme value statistics were used. Because the "correct" distribution function for the river system is not known a priori and may be subject to changes when the data basis changes, we use a selection of five different extreme value distribution functions: Gumbel, LogNormal, Generalized Logistic, Pearson III and Generalized Extreme Value (GEV) (Robson and Reed, 1999; Stedinger *et al.*, 1993). The functions are fitted to the data sets by the method of L-moments. The ability of the different functions to describe the characteristics of the data series was assessed by a maximum likelihood estimator. These estimators were used as weights to construct a composite distribution function from all five distributions (Wood and Rodriguez-Iturbe, 1975).

Because the shape of the flood wave has also a significant influence on the inundated area, normalised hydrographs were derived from the time series of the event associated to the annual maximum discharge. These normalised hydrographs were analysed by a cluster analysis yielding seven distinct flood types ranging from short single peak to long lasing multiple peak events. For details of this method see (Apel *et al.*, 2004).

3.2 Tributary inflow

A correlation analysis of the peak discharges of corresponding flood events of the Rhine and the tributaries showed a tight linear correlation. For this analysis the annual maximum discharge series of gauges Hattingen (Ruhr) and Schermbeck (Lippe) for the period 1961–1995 was selected. These correlations were used to drawn randomly correlated peak discharges for Ruhr and Lippe for each peak discharge in the Rhine (cf. Apel *et al.*, 2004).

In order to retain the dependency of the flood events in the Rhine and the tributaries, the normalised hydrographs of the tributaries were derived from the same time window as the event in the Rhine. By this method the time lag between peak discharges in Rhine and tributaries was preserved. Additionally, the clustering of the tributary hydrographs was identical to the clustering of the Rhine hydrographs, i.e., the clusters contain the corresponding hydrographs of the tributaries to the flood events in the Rhine. By this procedure the observed interplay of the flood waves in Rhine and tributaries was retained in the simulations. Consequently, in the Monte-Carlo analysis the cluster selected for the tributary hydrographs was the same as for the main river. Figure 2 shows the superposition of the standardised flood waves in Rhine and Ruhr and Lippe.

3.3 Flood routing and discharge-stage relation

The attenuation and translation of flood waves in the river reach was investigated by 1D-hydrodynamic simulations. I could be shown that these effects are negligible within this reach (Apel *et al.*, 2008). Therefore a flood routing for the translation of the flood waves was not performed in the model system. In order to test for dike overtopping the discharges had to be transformed into stages at each model breach location (see below) by discharge-stage relation curves. These were derived from a 1D-hydrodynamic model (HEC-RAS, (Brunner, 2002) of the Lower Rhine with cross sections every 500 m. The model was calibrated to the large flood event of 1995. An exponential regression model was fitted to the discharge-stage data given by the hydraulic model for every cross section. The discharges generated by the dynamic-probabilistic model were transformed into stage elevations at the model breach locations using these regression formulae in order to test for dike failures.

3.4 Dike failure, breach outflow and inundation area estimation

Dike failures could principally occur everywhere within the reach, because dikes protect from flooding everywhere except the few locations where natural high embankments are present. As a consequence this would induce that a risk assessment considering dike failures needs to test for dike failures all along the reach. However, this continuous test for dike failures would require enormous CPU-time and would not be suitable for a Monte-Carlo framework. Therefore scheme was developed, which test for dike failures in a quasi continuous way. These scheme is based on the idea of similarities of inundation patterns and areas caused by dike breaches along a certain segment of the dike lines. In order to determine these similar inundation patterns, 2D inundation simulations were performed every flow km to both sides of the river. Fore these simulations a constant breach width of 100 m and a constant outflow with water levels at the dike crest was assumed. The outflow through the breach was calculated by a standard formula for broad crested weirs. The assumed breach locations were grouped by their similarities in the associated inundation areas. The midpoint of each group of dike sections was assumed as a "model breach location" in the risk assessment. By this procedure 41 model breach locations were identified on both sides of the river along the complete reach (Fig. 1). More details about

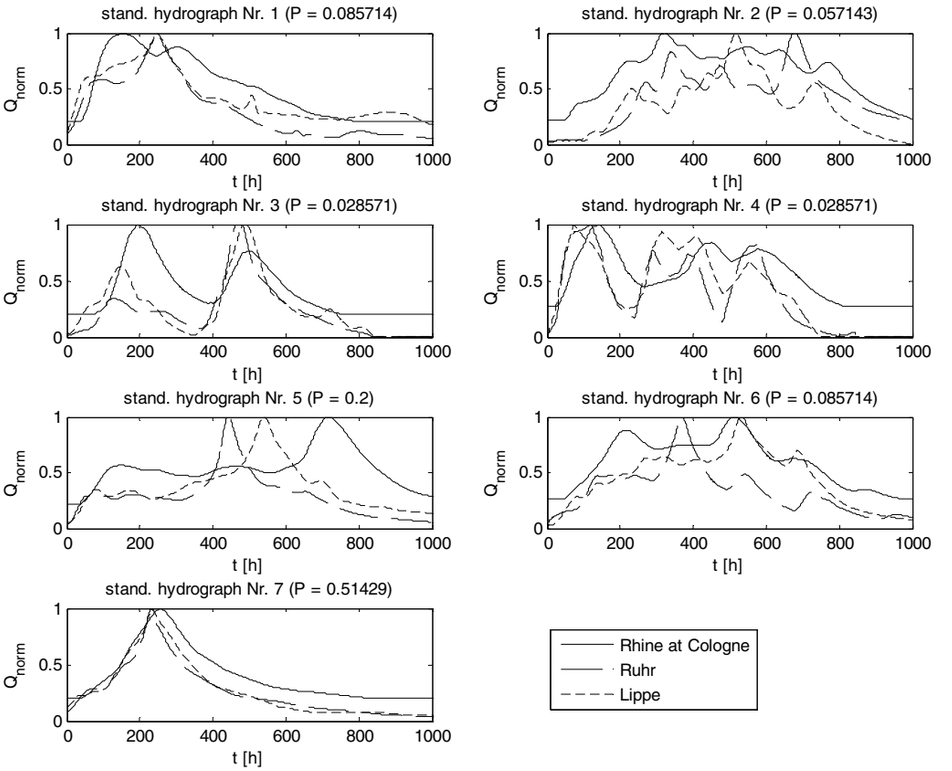

Figure 2 Superposition of the synthetic flood waves of the Rhine and the tributaries Ruhr and Lippe for the flood types identified in the cluster analysis. The flood waves are scaled in time, but normalised to flood peak. P denotes the probability of occurrence derived from the number of events in the respective cluster in relation to all 35 events. (Figure originally published in Apel *et al.*, 2008.)

the derivation of the model breach locations can be found in Apel *et al.* (2008).

At these model breach locations the test for dike failure was performed. For this conditional dike fragility curves were constructed, which determine the probability of failure conditioned by the overtopping height and duration of a flood wave over the dike crest. The method is an extension of the method proposed in (USACE, 1999) and is explained in detail in Apel *et al.* (2006, 2008).

Beside the water level in the river the width of the dike breach determines the outflow volume and hence the inundation area and depth in the hinterland. However, the determination of the breach width depends strongly on dike properties like material composition, geometry, construction type, maintenance, etc. is hence very difficult to calculate deterministically. Therefore we assessed the breach width based on a statistic of historical dike breaches at the Rhine in the period 1882–1883 (Merz *et al.*, 2004), where 14 breaches occurred. The mean breach width of 70.3 m was used for the risk assessment, whereas for the uncertainty assessment the standard deviation of 31.5 m was additionally taken into account (see section 5).

The outflow through a dike breach serves as the boundary condition for the estimation of the inundation extent and depths. However, 2D-inundation simulations could not be used within the Monte Carlo framework because of their high computational demand. Therefore inundation lookup tables were constructed for every model breach location by a priori 2D-inundation simulations with constant outflow approximating the outflow through a 100 m breach at water levels at dike crest elevation. These lookup tables relate distinct outflow volumes to the inundation depths within affected postal zones. This spatial aggregation was chosen, because the asset values for the damage estimation were available as aggregated mean values for postal zones only. For every postal zone the percentage of the whole area covered by the zone inundated to predefined stage intervals was recorded. The intervals were < 0.2m, 0.21–0.4m, 0.41–0.6m, 0.61–0.8m, 0.81–1.0m, 1.01–1.5m, 1.51–2.0m, 2.01–2.5m, 2.51–3.0m, 3.01–3.5m, 3.51–4.0m, 4.01–4.5m, and > 4.51m. This pre-processing step was the most demanding in terms of CPU-time of the whole analysis and was performed on a high performance computational Linux-cluster with 18 nodes. However, it has to be performed only once for a reach under study. Every following risk assessment using e.g., different asset values utilizes the same lookup tables.

For the damage estimation the area inundated to the defined inundation levels was interpolated from the lookup tables given the calculated cumulated outflow through the breach.

3.5 Damage estimation

In this study, the damage estimation is restricted to the damage at residential buildings. In the basic model a stage-damage function is applied that has been used in different flood risk mapping projects in Germany (ICPR, 2001, LfUG, 2005). The model is

suitable for applications on the meso-scale, i.e., for the application to land cover units. Damage at residential buildings is estimated by the relation $y = (2x^2 + 2x)/100$, where y is the damage ratio and x is the water level given in meter.

First, the function is combined with the estimation of inundation depths per land cover unit in order to determine damage ratios. These are then multiplied by the specific asset value assigned to each land cover unit. The total asset value of residential buildings is taken from the work of Kleist *et al.* (2006). Since only the sum of all residential assets is provided for each municipality, the assets were reallocated to postal zones. Within a postal zone the assets were concentrated on the settlement areas of the CORINE land cover data 2000 (CLC2000).

3.6 Monte Carlo framework

The modules described above are linked in a Monte Carlo simulation framework representing the flood process chain: generation of flood waves for the Rhine and the tributaries ⇒ superposition of the flood waves ⇒ transformation of discharges into stages at each model breach location ⇒ testing for dike failures ⇒ in case of failure calculation of breach outflow and reduction of the flood wave ⇒ and finally the calculation of the damage caused by the inundation of the hinterland. Figure 3 shows the flowchart of a single Monte-Carlo run of the model.

Within the Monte Carlo framework 10^5 model runs were performed, i.e., 10^5 synthetic flood events were created for the reach. this number of model runs proved to yield stable results for return periods up 1000 years. Model results are derived flood frequencies for every gauge within the reach and a cumulated risk curve for the whole river reach. Sections 6 and 7 present and discuss the results of the model in these terms. However, in this study, the derived flood frequencies at the end of the river reach, gauge Rees, is discussed only. A detailed discussion of the influence of dike breaches on the flood frequencies of downstream gauges can be found in Apel *et al.* (2008).

For the risk assessment of the whole river reach, a series of $n = 10^5$ damage estimates is calculated, which constitutes the risk curve for the complete reach. The return period T for each single damage estimate are empirically derived from the rank in the ordered data series. In this procedure the calculated damage values are sorted in ascending order, and the empirical occurrence probability is calculated using the rank r of the value in the series (1 for the lowest value and 10^5 for the largest) as follows:

$$T = \frac{1}{1 - (r/n + 1)} \tag{1}$$

In order to derive uncertainty estimates for the derived flood frequency curve at Rees and the risk curve a second level of Monte Carlo simulations was implemented. Within this level the various quantified uncertainty sources described in section 5 are randomised for selected return periods T. By this method uncertainty distributions for each T are derived, which are equivalent to variance estimations of the respective quantiles of the derived flood frequencies and risk curve. Figure 3 illustrates the modules considered in the uncertainty assessment, whereas section 5 gives details about the quantification and types of uncertainty sources considered, as well as about the method of combining the uncertainties in the model system.

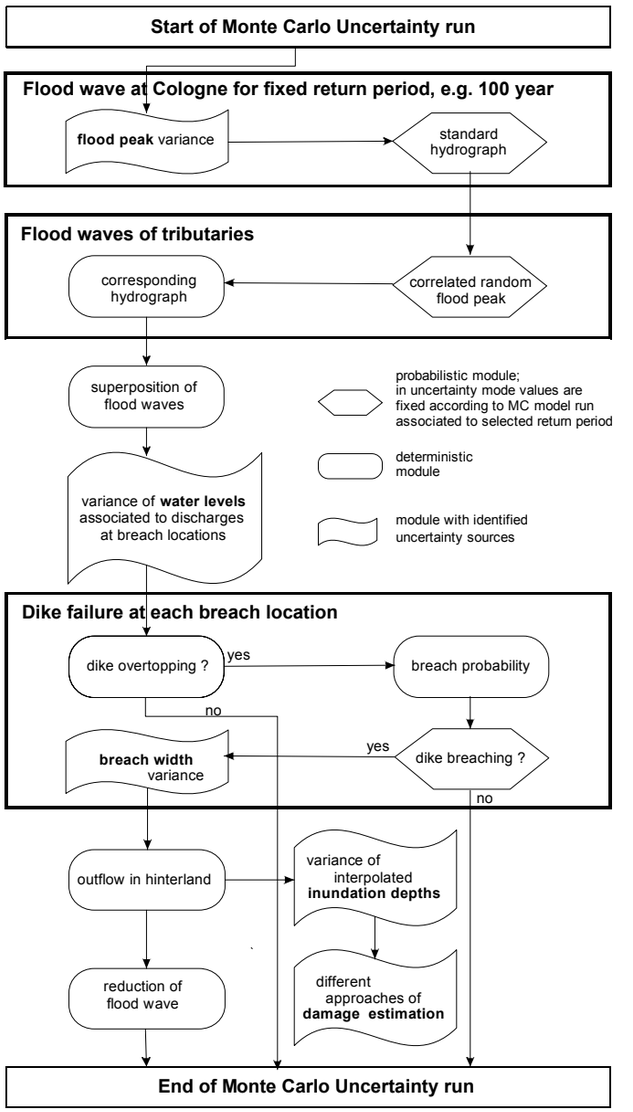

Figure 3 Flow chart of a single Monte Carlo run of the modelling system with distinction of deterministic, probabilistic and modules considered in the uncertainty assessment. (Figure taken from Apel *et al.*, 2008; modified to illustrate uncertainty assessment.)

4 Data series

For the hazard assessment the continuous and annual maximum discharge series (AMS) of the gauge Cologne (Rhine) of the period 1961–1995 was used. For the tributaries the discharge series of the flood events corresponding to the flood events in the Rhine were extracted from the records of the gauges Hattingen (Ruhr) and Schermbeck I (Lippe). The length of the series was determined by the length of the records at all three gauges and the fact that considerable structural hydraulic works were undertaken at the Rhine in the 1950's (Lammersen *et al.*, 2002).

In order to show the influence of the length of the data series on the uncertainty of flood risk assessments, a synthetic AMS of 1000 years length was derived on the basis of the recorded AMS 1961–1995 and a synthetic discharge series for the gauge Andernach upstream of Cologne. The synthetic series was derived from a 1000 year rainfall series generated by a stochastic rainfall simulator in combination with a hydrological model for the upper and middle Rhine. (Lammersen, 2004) published the 10 largest discharges of the resulting discharge series considering dike breaches along the Middle Rhine for the gauge Andernach. The 1000 year synthetic discharges series for Cologne was constructed according to the guideline of the German Association of Water Resources for the assimilation of historical flood records in discharge data series (DVWK, 1999). Utilizing this method, we interpreted the 10 synthetic discharges published by Lammersen and the two discharges of the recorded series larger than the smallest synthetic discharge as historical records. The remaining 988 records for the synthetic 1000 year series were drawn uniformly from the remaining recorded discharges thus creating a continuous record set with 1000 values. Figure 4 shows the fit of the different extreme value distributions using L-Moments to the recorded and synthetic AMS. It can be seen that the longer data series causes less spread of the different functions for rare events, i.e., for return periods $T > 100$ a.

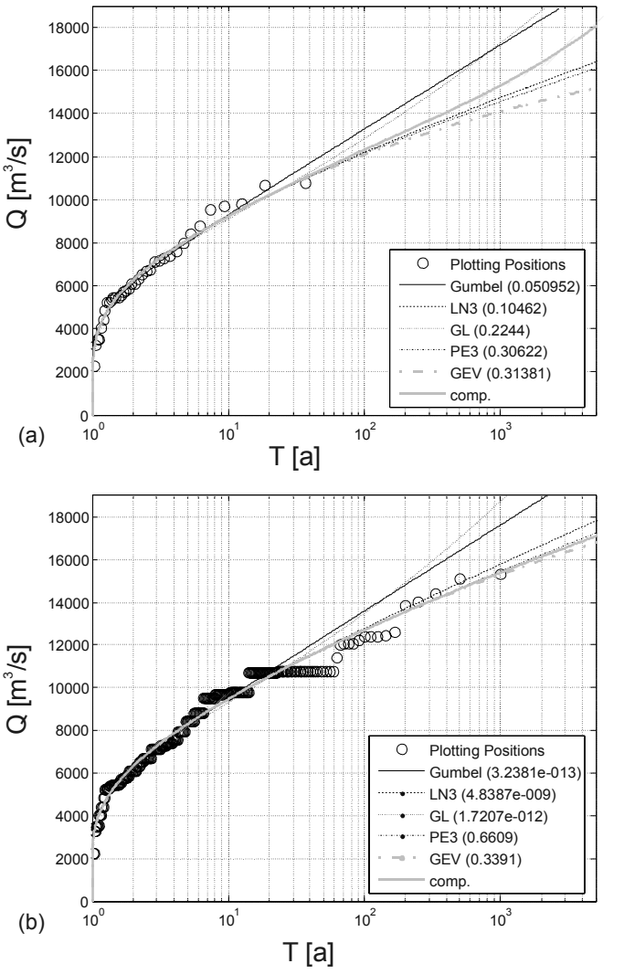

Figure 4 Fit of the selected extreme value distribution function and the weighed composite function for the (a) recorded (short) and (b) the synthetic AMS of Cologne. The numbers in brackets indicate the maximum likelihood weights.

5 Uncertainty sources

The final aim of this study is an estimate of the predictive uncertainty of the model, which includes data (DU), parameter (PU) and model (MU) uncertainties. According to (Merz and Thieken, 2005) the different uncertainty sources considered for the predictive uncertainty assessment can be categorised as epistemic. All three different types of uncertainty are treated simultaneously and equally weighed for the assessment of the predictive uncertainty. Table 1 lists the uncertainty sources considered along with a categorisation and short description of the quantification.

In line with the model setup, the uncertainty sources considered in this study can be separated into sources affecting the hazard and the vulnerability side of the risk assessment. On the hazard side the uncertainties caused by the estimation of the inflow into the modelled reach by EVS, the Q-H-relation transforming discharge into stages at the model breach locations and the width of an eventual dike breach are considered. For the final risk assessment the uncertainties in the interpolated inundation depths and the estimation of the damage ratio to buildings were additionally considered. Details about the quantification of the uncertainty source provide the following sections.

In order to derive an uncertainty assessment of the final products of the modelling system, the derived flood frequency statistic at Rees and the risk curves for the complete reach, it is necessary to assess the uncertainty for different return periods, i.e., quantiles of the resulting discharge and damage distributions. In this

Table 1 Uncertainty sources considered in the modelling system.

	Hazard (derived EVS)				Risk assessment	
Uncertainty source	Discharge series (DU)	Extreme value statistics (MU, PU)	Q-H-relation (PU)	Dike breach width (MU, PU, DU)	Inundation depths (DU)	Damage estimation (MU)
Quantification	two discharge series of different length	weighed combined variance of quantile estimators	variance of regression parameters	statistically by normal distribution with upper and lower bounds	variance of interpolated inundation depths	set of 3 different damage models

(DU = data uncertainty; PU = parameter uncertainty; MU = model uncertainty.)

study we selected the return periods of $T = 1.5$, 2, 5, 10, 20, 50, 100, 200, 500, 1000, 2000, 5000 and 10000 a. The general procedure of the uncertainty assessment is outlined as follows:

(1) randomisation of the discharges for the selected return periods at Cologne based on the variance of these quantiles,
(2) transformation of discharges into stages at the breach locations by randomised regression parameters of the Q-H-relation for the testing for dike failures,
(3) in case of a breach width randomisation of the breach width for the outflow calculation,
(4) superimposition of a random error on the interpolated inundation depth,
(5) application of three different damage models for the transformation of inundation depths to damage ratios.

Following this procedure an uncertainty distribution of discharges at Rees and cumulated damage in the reach for all selected return periods at Cologne is derived. These distributions are drawn in the derived flood frequency statistics and risk curves at appropriate locations. The locations are determined by tracing the discharge of the selected return period of the input series in the sorted output series. This is necessary because e.g., a 1000-year discharge at the input is not necessarily the 1000-year discharge in the output series due to possible dike breaches and randomised tributary inflow. By this procedure it is guarantied that the uncertainty distributions are drawn at the correct location of the derived flood frequency and risk curves. The following sections describe the different uncertainty sources and their combination in detail.

5.1 Extreme value statistics and distribution functions

The variance of quantile estimators for the selected extreme value functions was quantified by a bootstrapping approach. The respective data series used was resampled 1000 times to the original length and the extreme value functions fitted by L-moments. The variance of the quantile estimators was estimated from the resulting data set of quantile predictors of the different functions. Figure 5 shows the variance of the quantile estimators of the extreme value distribution functions in terms of a 95% confidence intervals for both the recorded (short) and synthetic AMS. The reduction of the variance of estimators of extreme events using a longer time series is clearly visible for all functions.

The variance of the quantile estimators of the composite distribution was derived by random sampling of quantile estimators of the extreme value functions based on the variance derived from the confidence intervals. Under the assumption of normal distribution the standard deviation to each quantile estimator was calculated from the confidence intervals. Using these standard deviations a set of 10^4 random samples was assembled for every quantile of the composite distribution. Every extreme value function contributed a number of samples to the overall 10^4 according to the maximum likelihood weights of the goodness of fit test (cf. section 3.1). These composite random discharge sets provided an estimate of the variance of the quantiles of the composite distribution function.

5.2 Discharge-stage relation

The discharge-stage relation at each model breach location is described by an exponential regression model fitted to

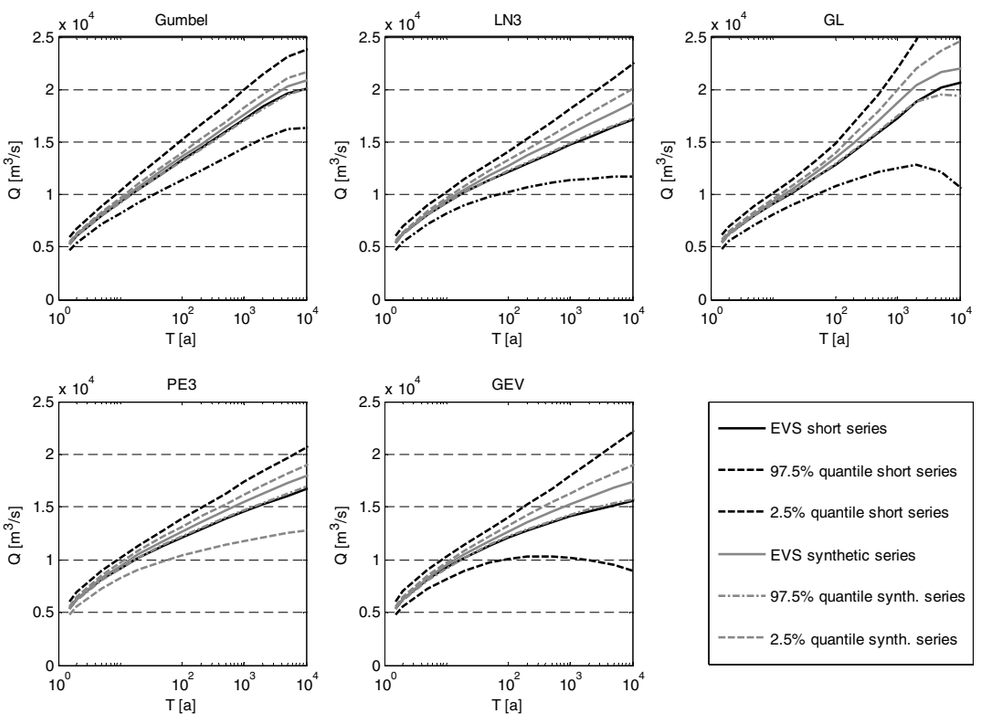

Figure 5 95% confidence intervals of the extreme value distribution functions for the recorded (short) and synthetic AMS derived by resampling of the original data set.

discharge-stage data given by a 1D hydraulic model of the lower Rhine (Fig. 6, small panel). The function used was:

$$H = a \times \exp(b \times Q) + c \times \exp(d \times Q) \quad (2)$$

with a, b, c, d as regression parameters.

The error estimate for the translation of discharges into stages is derived from the confidence intervals of the parameters of the regression. Under the assumption of normal distributed parameter errors standard deviations for all four parameters were derived, which were consequently used for the randomisation of the parameters. Figure 6 shows the effect of the parameter uncertainty on the discharge-stage relationship in terms of a 95% confidence interval exemplarily for model breach location #1. The confidence interval was calculated by a Monte Carlo analysis varying the regression parameters, whereby the regression parameter space was sampled by a Latin Hypercube scheme with 80 quantile divisions.

5.3 Breach width

The width of a dike breach is hard to predict, because of the complex breaching mechanisms, insufficient knowledge about the processes itself and their modelling and most of all because of the absence of detailed structural and geometric data of the dikes. Therefore and because of the large influence of the breach on the extent of the inundation area, the breach width is a considerable uncertainty factor. Because of the lack of knowledge about breach formation the width was assumed as normal distributed random process, with mean and variance given in section 3.4. In order to obtain reasonable breach widths in the randomisation, the distribution was bounded at the lower end to the smallest recorded value (35 m) and to 200 m at the upper end, which is an expert judgement about maximum breach widths in the investigation area.

For the risk assessment the breach width was kept constant at the mean value (70.4 m). However, for the uncertainty assessment the width was randomised assuming a normal distribution with the standard deviation of 31.5 m in order to assess the uncertainty caused by variations in the breach development.

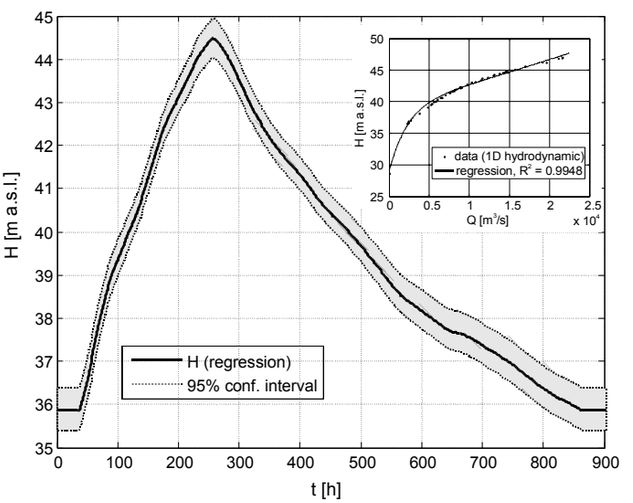

Figure 6 Uncertainty caused by Q-H-relation for model breach location #1.

5.4 Inundation depths

Errors in inundation simulations mainly origin in errors in the underlying DEM and incorrect ground surface roughness parameterization (Bates *et al.*, 2003; Mason *et al.*, 2003). Assuming a well calibrated hydraulic model, the uncertainty of the inundation predictions can be derived by putting a random error representing the accuracy of the DEM on the elevation points used in the model and run the model in a Monte Carlo framework. However, this approach is not viable with the proposed model structure, since the inundation depth are not simulated explicitly every model run, but interpolated from the inundation tables (cf. section 3.4). Therefore the interpolated inundation depths were modified with a random error within every postal zone. The random error was assumed normally distributed with mean $\mu = 0$ m and a standard deviation of $\sigma = 0.5$ m. This assumption is based on the error estimate of 1 m of the DEM in lowland areas given by the land survey authorities. This error estimate is mapped in the uncertainty assessment by imposing a random error on the simulated inundation depths. This method does not take the effects of a different topography on the inundation process into account, but it gives a rough estimate about possible errors in the inundation simulation caused by errors in the DEM.

5.5 Damage estimation

The uncertainty of the damage estimation is dominated by model uncertainty. At present no universally accepted damage model exists for damage estimations in Germany, resp. North-Rhine Westphalia. In order to assess the uncertainty caused by the translation of inundation depth into relative damage to buildings, we applied three different damage models, all developed for North-Rhine Westphalia, resp. the whole catchment of the Rhine, and evaluated the range of damage ratio predictions given by the different models. All three models define a functional relationship between inundation depth and damage ratio. The functions used were:

(1) The damage function of the International Commission for the Protection of the Rhine (ICPR, 2001),
(2) a linear damage function developed by the Ministry of Environment, Spatial Planning and Agriculture of North-Rhine Westphalia MURL (2000), and
(3) the square root damage function developed by HYDROTEC (2001) consulting civil engineers.

Figure 7 shows a comparison of the different function in terms of damage ratio related to inundation depth. The absolute damage is achieved by combing the damage ratios with the assets of residential buildings given by Kleist *et al.* (2006) that were disaggregated within the postal zones (see section 3.5).

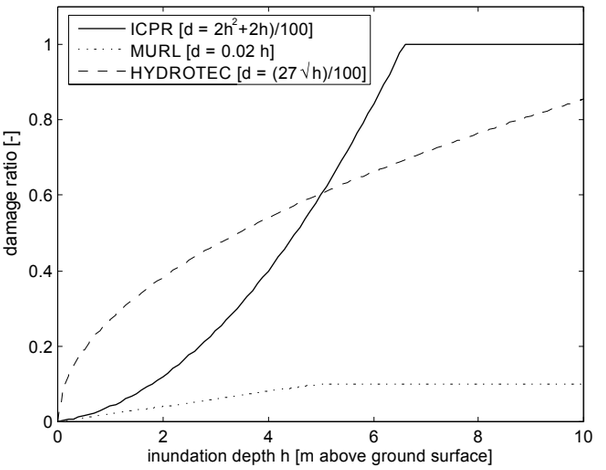

Figure 7 Damage functions used for the uncertainty assessment.

5.6 Combination of uncertainty sources

Since the model system separates the hazard and vulnerability part of the risk assessment, the uncertainty assessment is also splitted in two parts: The first part considers the uncertainties affecting the hazard, i.e., the uncertainties caused by the EVS, the Q-H-relation and the breach width. These uncertainty sources can be analysed separately or in various combinations analogously to a sensitivity analysis as presented e.g., in (Hall *et al.*, 2005b; Pappenberger *et al.*, 2006a; Pappenberger *et al.*, 2006b). In order to reduce computation time, a Latin Hypercube Sampling with $n = 80$ quantile divisions was applied for each selected return interval. The hypercube dimension ranged from $n \times 1$ to $n \times 5$ depending on the uncertainty sources considered.

In the second part, i.e., the uncertainty assessment of the risk estimates, a random error was superimposed on the interpolated inundation depths according to section 5.4. Finally, the resulting building damage was calculated with all three damage functions. This results in 240 damage estimates per selected return interval, which were all used without any weighting in the uncertainty assessment thus including the model uncertainty of the damage estimation.

6 Results

The proposed uncertainty assessment method allows the distinctive assessment of the influence of single uncertainty sources as well as various combinations of different sources. However, we focus on the comparison of the total predictive uncertainty, i.e., the combination of all considered sources, to the uncertainties caused by single sources alone. Figure 8 shows the results obtained for the derived extreme value statistic at gauge Rees, i.e., the predicted hazard, for the recorded AMS 1961–1995. It can be shown that the predictive uncertainty considering all sources is comparatively high, with rising uncertainty for extreme events, as expected: the more it is extrapolated beyond the length of the data series to extreme events, the higher gets the uncertainty of the predictions. Analysing the uncertainties caused by the different single sources, it can be seen that the total uncertainty associated to lower return intervals is exclusively caused by the extreme value distributions, whereas the uncertainty of the higher return intervals is composed of all hazard relevant sources, with uncertainties caused by the distributions and Q-H-relation almost equally high. The range of the uncertainty caused by the breach width is approximately half of the range of the others. However, the single uncertainties are not additive. The total uncertainty range is only slightly higher than considering the uncertainty by distributions or Q-H-relation separately. This implies that the single uncertainties partially compensate each other when combined.

Figure 9 shows the equivalent graphics as Fig. 8 but for the synthetic AMS. Using this data series, the uncertainty caused by the distributions is significantly reduced, especially for the more frequent events. However, the total uncertainty associated to large discharges is only slightly lower than for the short series, because the uncertainty caused by the Q-H-relation is still considerable for large events.

The results of the uncertainty assessment for the risk curves generally show a similar behaviour than for the derived extreme value statistics. The obvious differences can be explained by the additional uncertainty sources and the model characteristics: The comparatively larger reduction of the total uncertainty using the long synthetic AMS (Figs 10 and 11) can be attributed to the additional uncertainty imposed by the damage models. Because of the large differences of the predicted damage ratio (cf. Fig. 7) a wide range of damage values is predicted by the different damage models. Therefore even small changes of the inundation depths have a large impact on the predicted damage range.

Another difference is the lack of uncertainty for low return periods. This is caused by the model setup calculating damage in case of dike breaches only. Up to a certain discharge level the model predicts no dike breaches and consequently no damage. For low return periods even the largest discharge in the uncertainty range is lower than the breach threshold, i.e., the water stage is below the dike crest und hence the uncertainty estimate equals zero.

Surprisingly the errors imposed on the inundation depths cause only small uncertainties. This is possibly an effect of the independent randomisation of the inundation error for every postal zone, which may result in an averaging of the imposed errors to the mean, i.e., 0.

7 Discussion

The proposed model system and uncertainty quantification approach is able to provide a derived flood frequency statistic and a probabilistic cumulated risk assessment for a complete river reach, both based on process based models which are embedded into a probabilistic framework. Moreover, the system allows for a comparative uncertainty assessment of different relevant uncertainty sources. Using these capabilities a total predictive uncertainty assessment could be performed. Moreover, the major sources of uncertainty could be identified. The major sources

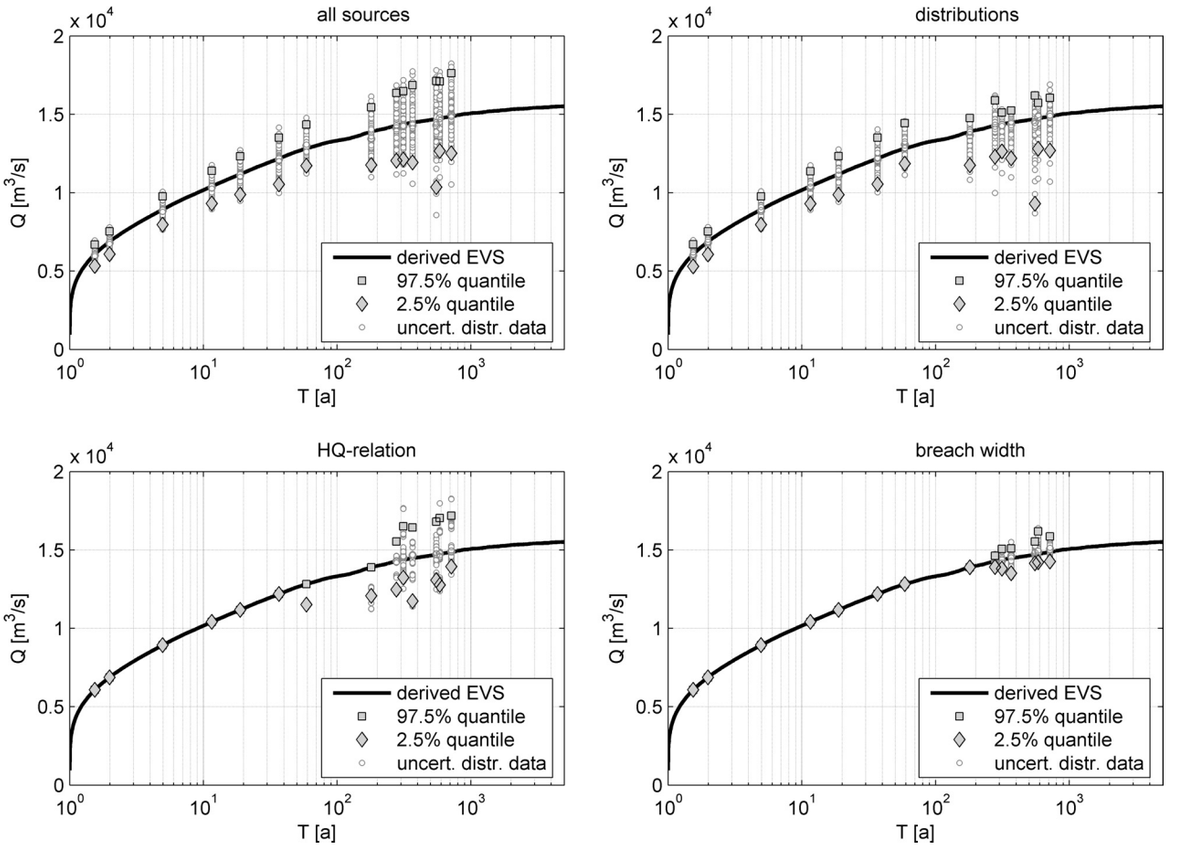

Figure 8 Uncertainty of the derived extreme value statistic of gauge Rees caused by different sources for the AMS 1961–1995 of Cologne.

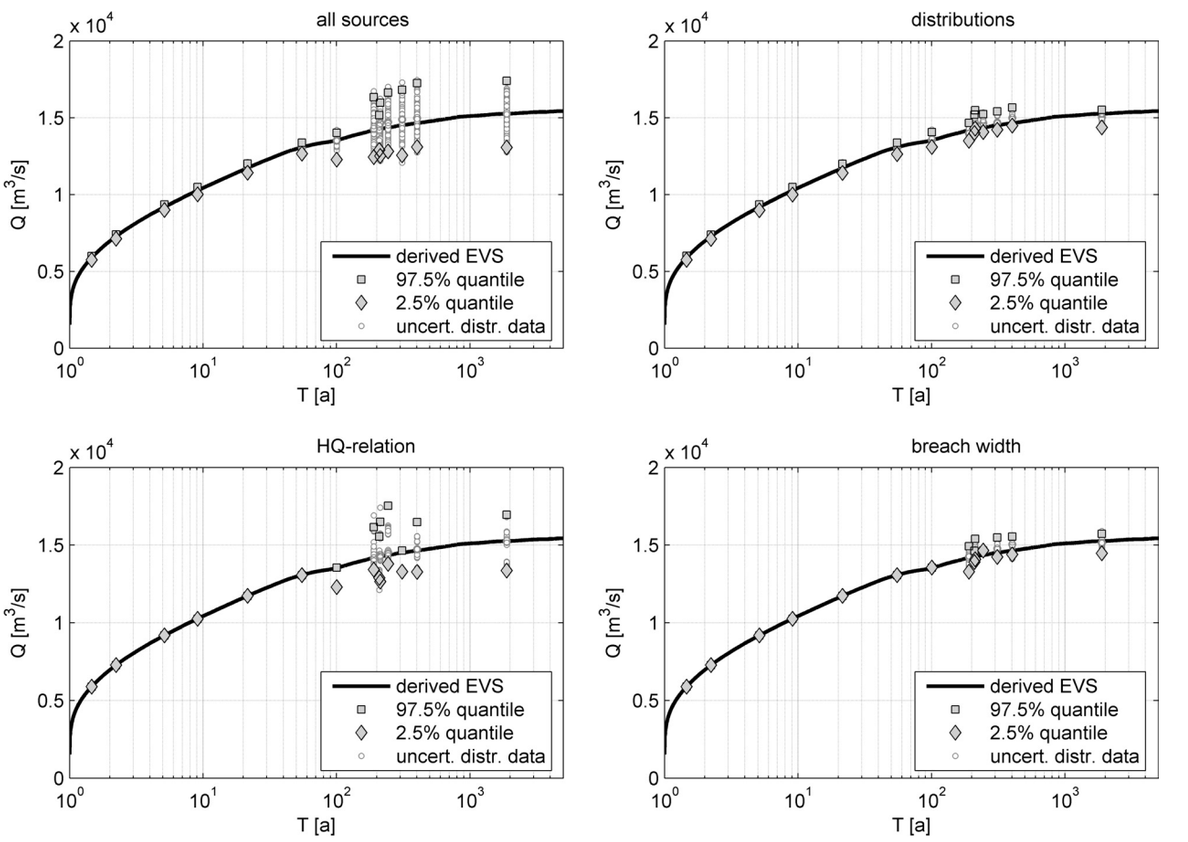

Figure 9 Uncertainty of the derived extreme value statistic of gauge Rees caused by different sources for the 1000 year synthetic AMS of Cologne.

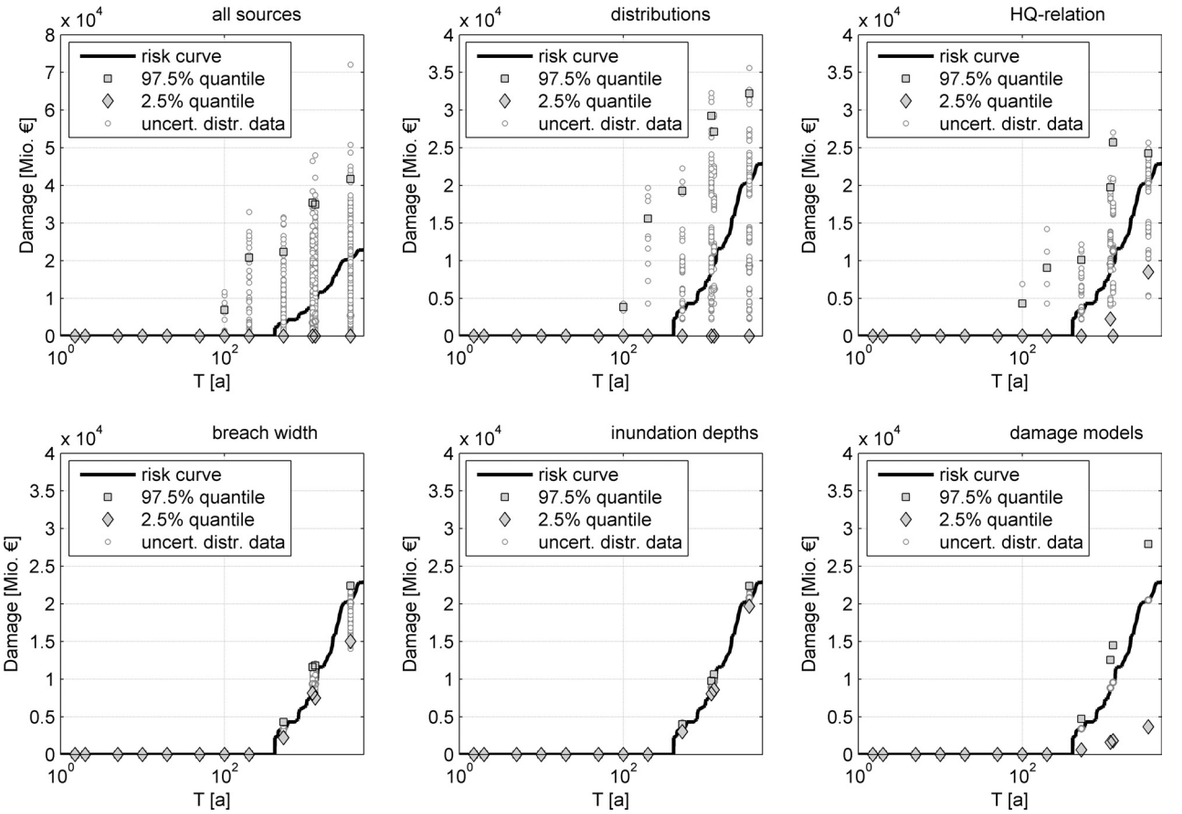

Figure 10 Uncertainty of the risk curve for the Lower Rhine caused by different sources for the AMS 1961–1995 of Cologne (note the different scale for "all sources").

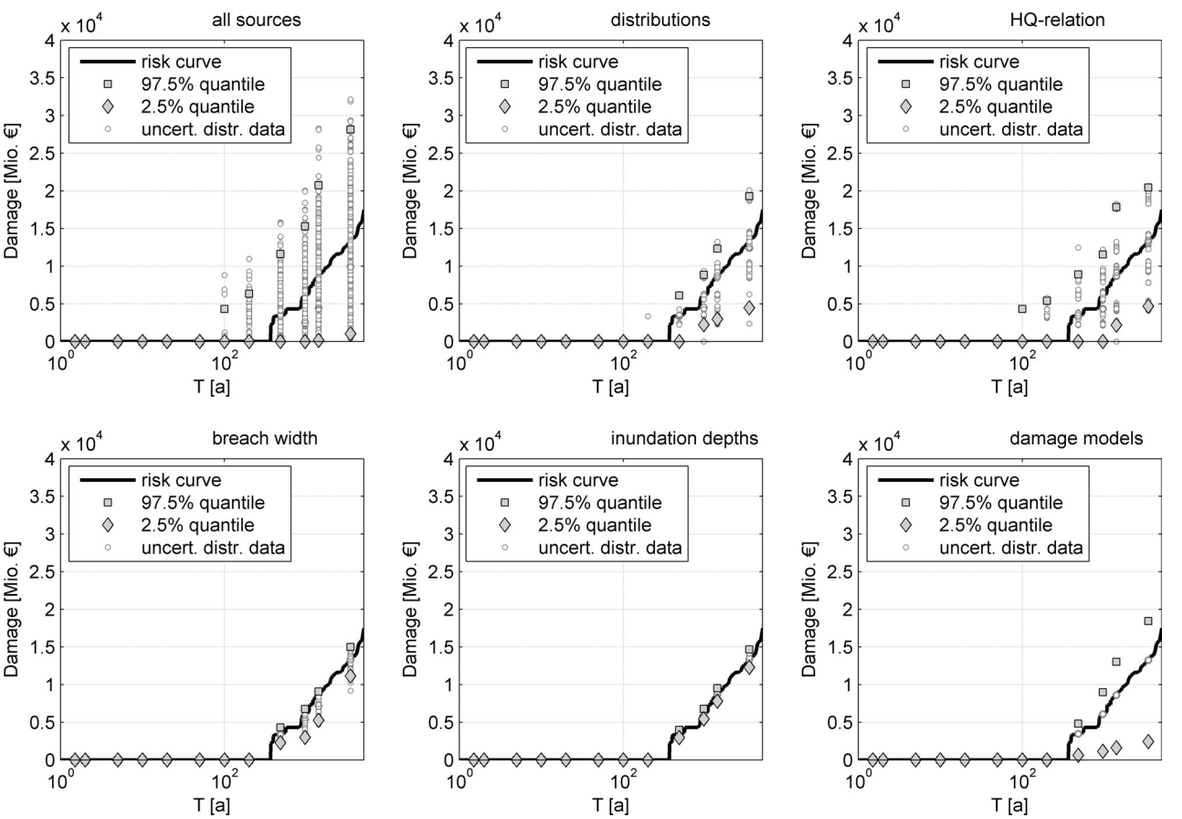

Figure 11 Uncertainty of the risk curve for the Lower Rhine caused by different sources for the 1000-year synthetic AMS of Cologne.

of the hazard assessment part of the risk assessment were the model and data uncertainty of the extreme value statistics and the used AMS and the uncertainty of the Q-H-relation. For the final risk assessment the model uncertainty of the damage estimation proved to be another significant uncertainty source, which produced an uncertainty range almost equal to the uncertainty by distribution and Q-H-relation.

However, the combination of the single uncertainty sources showed that they are not strictly additive, but compensate each other to some extent. This implies that a reduction of one of the major uncertainty sources does not necessarily reduce the total predictive uncertainty. In order to reduce the total uncertainties all the three major uncertainty sources have to be reduced for a reduction of the overall predictive uncertainty.

The uncertainty assessment presented here considered a comparatively large number of uncertainty sources, however it cannot be regarded as complete in a sense that all possible uncertainty sources were considered or described in a satisfactory way. For example, the uncertainties caused by the roughness parameterisation for the a priori inundation simulations or the 1D model for the Rhine were not taken into account explicitly. A detailed study as e.g., performed in (Pappenberger *et al.*, 2005a) would possibly lead to a more realistic assessment of the uncertainty caused by the Q-H-relation as presented here. The selection of the uncertainty sources was based on the expert judgement of the authors and thus subjective. It would be surely worthwhile to discuss the inclusion of additional uncertainty sources in future studies, which would be feasible with the proposed method. However, this study showed that sources considered cause large uncertainties in flood risk assessments already. In order to increase the reliability of flood risk assessments the identified main sources of uncertainty should be reduced.

References

1. AMENDOLA, A. (2001). "Recent Paradigms for Risk Informed Decision Making," *Safety Research*, 40, 17–30.
2. APEL, H., MERZ, B. and THIEKEN, A.H. (2008). "Influence of Dike Breaches on Flood Frequency Estimation," *Computers and Geosciences*,article in press, doi: 10.1016/j.cageo.2007.11.003.
3. APEL, H., THIEKEN, A.H., MERZ, B. and BLÖSCHL, G. (2004). "Flood Risk Assessment and Associated Uncertainty," *Natural Hazards and Earth System Science*, 4(2), 295–308.
4. APEL, H., THIEKEN, A.H., MERZ, B. and BLÖSCHL, G. (2006). "A Probabilistic Modelling System for Assessing Flood Risks," *Natural Hazards*, 38(1–2), 79–100.
5. BATES, P.D., MARKS, K.J. and HORRITT, M.S. (2003). "Optimal Use of High-Resolution Topographic Data in Flood Inundation Models," *Hydrological Processes*, 17(3), 537–557.
6. BRUNNER, G.W. (2002). *HEC-RAS River Analysis System - Hydraulic Reference Manual*, CPD-69, US Army Corps of Engineers – Hydrologic Engineering Center (HEC), Davis.
7. DVWK (1999). *Statistische Analyse von Hochwasserabflüssen*, Wirtschafts- und Verlags-Gesellschaft Gas und Wasser, Bonn.
8. FELTER, S. and DOURSON, M. (1998). "The Inexact Science of Risk Assessment (and Implications for Risk Management)," *Human and Ecological Risk Assessment*, 4(2), 245–251.
9. HALL, J.W., SAYERS, P.B. and DAWSON, R.J. (2005a). "National-Scale Assessment of Current and Future Flood Risk in England and Wales," *Natural Hazards*, 36(1–2), 147–164.
10. HALL, J.W., TARANTOLA, S., BATES, P.D. and HORRITT, M.S. (2005b). "Distributed Sensitivity Analysis of Flood Inundation Model Calibration," *Journal of Hydraulic Engineering*, 131(2), 117–126.
11. KELMAN, I. (2002). "Physical Flood Vulnerability of Residential Properties in Coastal, Eastern England," PhD Thesis, University of Cambridge, U.K., http://www.ilankelman.org/phd.html.
12. LAMMERSEN, R. (2004). *Grenzüberschreitende Auswirkungen von extremem Hochwasser am Niederrhein, Abschlussbericht*, Ministerium für Umwelt und Naturschutz, Landwirtschaft und Verbraucherschutz des Landes Nordrhein-Westfalen (MURL), Düsseldorf.
13. LAMMERSEN, R., ENGEL, H., VAN DE LANGEMHEEN, W. and BUITEVELD, H. (2002). "Impact of River Training and Retention Measures on Flood Peaks Along the Rhine," *Journal of Hydrology*, 267(1–2), 115–124.
14. MASON, D.C., COBBY, D.M., HORRITT, M.S. and BATES, P.D. (2003). "Floodplain Friction Parameterization in Two-Dimensional River Flood Models using Vegetation Heights Derived from Airborne Scanning Laser Altimetry," *Hydrological Processes*, 17(9), 1711–1732.
15. MERZ, B., APEL, H. and GOCHT, M. (2004). "Entwicklung eines probabilistischen Ansatzes zur Bestimmung des Deichversagens durch Überströmen," in MERZ, B. and APEL, H. (eds.), Risiken durch Naturgefahren, Scientific Technical Report STR04/01. GeoForschungsZentrum Potsdam, Potsdam, pp. 77–84.
16. MERZ, B. and THIEKEN, A.H. (2004). "Flood Risk Analysis: Concepts and Challenges," *Osterreichische Wasser und Abfallwirtschaft*, 56(3–4), 27–34.
17. MERZ, B. and THIEKEN, A.H. (2005). "Separating Natural and Epistemic Uncertainty in Flood Frequency Analysis," *Journal of Hydrology*, 309(1–4), 114–132.
18. PAPPENBERGER, F., BEVEN, K., HORRITT, M. and BLAZKOVA, S. (2005a). "Uncertainty in the Calibration of Effective Roughness Parameters in HEC-RAS Using Inundation and Downstream Level Observations," *Journal of Hydrology*, 302(1–4), 46–69.
19. PAPPENBERGER, F. et al. (2005b). *Risk & Uncertainty – Tools and Implementation*, Flood Risk Management Research Council FRMRC, Lancaster.
20. PAPPENBERGER, F., IORGULESCU, I. and BEVEN, K.J. (2006a). "Sensitivity Analysis Based on Regional Splits and

Regression Trees (SARS-RT)," *Environmental Modelling & Software*, 21(7), 976–990.

21. PAPPENBERGER, F. et al. (2006b). "Influence of Uncertain Boundary Conditions and Model Structure on Flood Inundation Predictions," *Advances in Water Resources*, 29(10), 1430–1449.
22. ROBSON, A. and REED, D. (1999). "Statistical Procedures for Flood Frequency Estimation," *Flood Estimation Handbook*, Vol. 3, Institute of Hydrology, Wallingford, UK, 338 p.
23. STEDINGER, J.R., VOGEL, R.M. and FOUFOULA-GEORGIOU, E. (1993). "Frequency Analysis of Extreme Events," in MAIDMENT, D.R. (ed.), *Handbook of Hydrology*, McGraw-Hill, New York, pp. 18.1–18.66.
24. USACE, 1999. *Risk-Based Analysis in Geotechnical Engineering for Support of Planning Studies. Engineer Technical Letter (ETL) 1110–2-556*, U.S. Army Corps of Engineers, Washington D.C.
25. WOOD, E.F. and RODRIGUEZ-ITURBE, I. (1975). "A Bayesian Approach to Analyzing Uncertainty Among Flood Frequency Analysis," *Water Resources Research*, 11(6), 839–843.
26. ZIO, E. and APOSTOLAKIS, G.E. (1996). "Two Methods for the Structured Assessment of Model Uncertainty by Experts in Performance Assessments of Radioactive Waste Repositories," *Reliability Engineering and System Safety*, 54, 225–241.